Structure and dielectric properties of Lu-doped SrBi2Ta2O9 synthesized by the molten salt method

Mohamed Afqir, Didier Fasquelle, Amina Tachafine, Yingzhi Meng, Mohamed Elaatmani, Abdelouahad Zegzouti, Abdelhamid Oufakir, Mohamed Daoud

Processing and Application of Ceramics 17 [3] (2023) 256–263
https://doi.org/10.2298/PAC2303256A

Structure and dielectric properties of Lu-doped $SrBi_2Ta_2O_9$ synthesized by the molten salt method

Mohamed Afqir[1,*], Didier Fasquelle[2], Amina Tachafine[2], Yingzhi Meng[3], Mohamed Elaatmani[1], Abdelouahad Zegzouti[1], Abdelhamid Oufakir[1], Mohamed Daoud[1]

[1]*Laboratoire des Sciences des Matériaux et optimisation des procédés, Faculté des Sciences Semlalia, Université Cadi Ayyad, Marrakech, Morocco*
[2]*Unité de Dynamique et Structure des Matériaux Moléculaires, Université du Littoral Côte d'Opale, Calais, France*
[3]*Guilin University of Technology, Guilin 541006, China*

Received 9 March 2023; Received in revised form 15 May 2023; Accepted 29 July 2023

Abstract

Lu-doped $SrBi_2Ta_2O_9$ ($SrBi_{2-x}Lu_xTa_2O_9$ where x = 0, 0.025, 0.05, 0.75 and 0.1) powders were synthesized by combination of molten salt method and solid-state route. FTIR, Raman and XRD techniques were performed to follow the transformation of reactants into the desired products. Characterization of all samples shows pure and single-phase orthorhombic structured materials obtained with plate-like morphology that is composed of fine and coarse-grained particles. The prepared powders were pressed and sintered at different temperatures up to 1200 °C. Microstructure of the sintered samples is also likely to be affected by doping. The first study of dielectric measurements describes the effect of the application of DC bias, at room temperature, on the undoped and Lu-doped ceramics and shows that there is little or no effect of DC bias. The sample $SrBi_{1.95}Lu_{0.05}Ta_2O_9$ had maximal dielectric constant (ε′) and minimal dielectric loss (tanδ). In the second part of this work, the temperature dependence of ε′ and tanδ was considered. It was concluded that Lu-doping not only reduces the Curie temperature, but also brings a diffused phase transition, showing a crossover between displacive and diffusive behaviour.

Keywords: *molten salt, diffuseness, dielectrics, microstructure, AC and DC conductivity*

I. Introduction

Early research on compounds with Aurivillius phase started in the 1940s. One of the most attractive materials from this group is strontium bismuth tantalate ($SrBi_2Ta_2O_9$), which shows no polarization fatigue with electric field cycling and has been very successfully applied in FeRAM [1,2]. However, the biggest challenge for commercially viable $SrBi_2Ta_2O_9$-based electronic devices is how to assess and enhance the electrical and dielectric properties [3,4].

The enhanced physical properties cannot be achieved only by doping, but also by choosing an adequate synthesis process. Compared with the huge energy consumption of the solid state process, chemical synthesis provides an appealing route under mild conditions. However, it still faces challenges in producing high-purity materials based on the $SrBi_2Ta_2O_9$ compound. Very few materials have been synthesized through the molten-salt route, largely because the current method involves additional chemicals arising from the molten mixture that may contaminate the materials, but also involves many steps in the synthesis process, which is time-consuming. Recently, we have proven that the molten salt technique is a promising method to prepare different Aurivillius compounds [5,6]. Substitution of ions in these complex structures is a popular technique to achieve desired material properties [7]. If the substitution is performed on Sr site, it favours the structural distractions in the TaO_6 octahedron that improves the ferroelectric behaviour, as observed in the enhancement of ferroelectric properties [1,8]. However, if the site of substitution is Ta, this leads to the enhancement

*Corresponding author: tel: +212 701231987,
e-mail: *mohamed.afqir@yahoo.fr*

of dielectric properties. Enhanced electrical and optical properties have been achieved by partially replacing Bi^{3+} ions in this oxide with mainly rare earth elements, such as Sm^{3+}, Eu^{3+} or Gd^{3+} [9–12].

The purpose of this study was to optimize the structure of Lu-doped $SrBi_2Ta_2O_9$ by changing the dopant content and sintering temperature in order to improve physical properties. To this end, the work consists of two parts: collecting the evidence of structural and microstructural characteristics and conducting quantitative measurements of dielectric properties.

II. Experimental

Lu-doped $SrBi_2Ta_2O_9$ ($SrBi_{2-x}Lu_xTa_2O_9$ where x = 0, 0.025, 0.05, 0.75 and 0.1) powders were synthesized using the stoichiometric amounts of $SrCO_3$ (99.9%, Aldrich), Ta_2O_5 (99.9%, Aldrich), $Bi_2O_2CO_3$ (99%, Aldrich) and Lu_2O_3 (99.5%, Acros Organics). The precursors were heated at 600 °C for 6 h and then ground manually for 30 min. The ground mixture was stirred for 3 h in the molten salt mixture containing 46 wt.% $NaNO_3$ and 54 wt.% KNO_3 to promote the crude powders. FTIR (VERTEX 70v FT-IR), Raman (Confotec, 532 nm), and XRD (SmartLab SE, Rigaku) techniques were performed to track the transformation of reactants into desired products. The obtained crude powders were heated at 1000 °C for 12 h in an electric furnace and then uniaxially pressed at 1 MPa to form pellets having thickness and diameter of 0.9 and 10 mm, respectively. The pressed pellets were sintered in air at different temperatures up to 1200 °C. Silver paste electrodes were fixed on both surfaces of the sintered pellets and fired at 400 °C for 20 min in air. XRD patterns were recorded in the 2θ range of 10–70° with a step of 0.05°. Scanning electron microscope SEM (TESCAN VEGA) was used to analyse microstructure on the cross section areas of the prepared ceramics. Dielectric measurements were carried out using Solartron 1260 impedance/gain-phase and IVYTECH LACR-106x analysers.

III. Results and discussion

3.1. Microstructure

XRD patterns of the synthesized $SrBi_2Ta_2O_9$ and $SrBi_{2-x}Lu_xTa_2O_9$ powders (in Fig. 1) are almost identical. They are isostructural with the $SrBi_2Ta_2O_9$ phase as compared with the XRD patterns in the ICDD database. All the diffraction peaks can be indexed to the $SrBi_2Ta_2O_9$ structure based on the orthorhombic crystal system with the $A2_1am$ space group. It can be observed that specific fingerprint peaks, corresponding to (113), (115), (020) and (135) planes, are easily identifiable in all XRD patterns. Thus, the used synthesis strategy can produce homogeneous materials with the resulting final products free from impurities.

If considering substitution of Bi^{3+} (1.02 Å) by Lu^{3+} (0.85 Å) ions with this large mismatch in ionic radii, one would have expected lower lattice parameters. However, the calculations reported in Table 1 revealed the smooth change of unit cell parameters upon adding Lu ions. It is important to underline that these physical values have an accuracy of measurement associated with them. Here, XRD data acquisition options only allowed us to determine the compounds' fineness as a primary purpose. In this regard, Lu-doping has not shown a significant change in structure.

Theoretical (ρ_{th}) and experimental (ρ_{ex}) densities were estimated through the XRD method and the Archimedes method, respectively (Table 1). Densities of the ceramics sintered at 1120 °C for 6 h are lower than that for the samples sintered at higher temperatures. The sintering at 1120 °C is not effective in getting a high density of ceramics, leading to lower fracture toughness and brittleness. It is demonstrated that sintering at 1200 °C maximizes experimental density, but at this

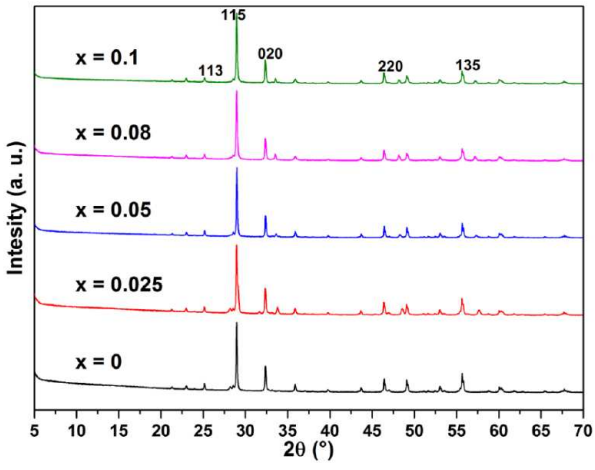

Figure 1. XRD patterns of Lu-doped $SrBi_2Ta_2O_9$ powders

Table 1. Cell parameters, theoretical density (ρ_{th}), experimental density (ρ_{ex}) at different sintering times and temperatures, and crystallite size (D) of Lu-doped $SrBi_2Ta_2O_9$

Composition	Cell parameters				ρ_{ex} [cm^3/g]			ρ_{th}	D [nm]
	a [Å]	b [Å]	c [Å]	V [Å^3]	1120 °C/6 h	1180 °C/8 h	1200 °C/1 h	[cm^3/g]	
x = 0	5.5239	5.5225	24.9853	762.1994	8.060	7.692	8.260	8.81	70
x = 0.025	5.5282	5.5285	24.9910	763.7941	8.010	8.016	8.190	8.79	70
x = 0.05	5.5249	5.5251	24.9880	762.7771	7.600	8.341	8.190	8.79	70
x = 0.075	5.5227	5.5229	24.9795	761.9057	8.160	8.349	8.340	8.80	70
x = 0.1	5.5264	5.5259	24.9868	763.0545	8.000	8.444	8.270	8.78	70

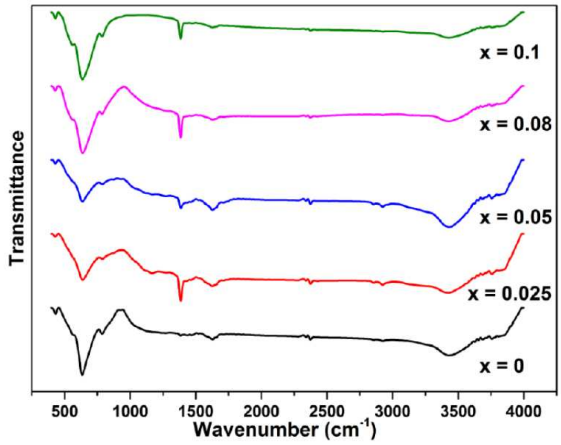

Figure 4. FTIR spectra of Lu-doped $SrBi_2Ta_2O_9$ powders

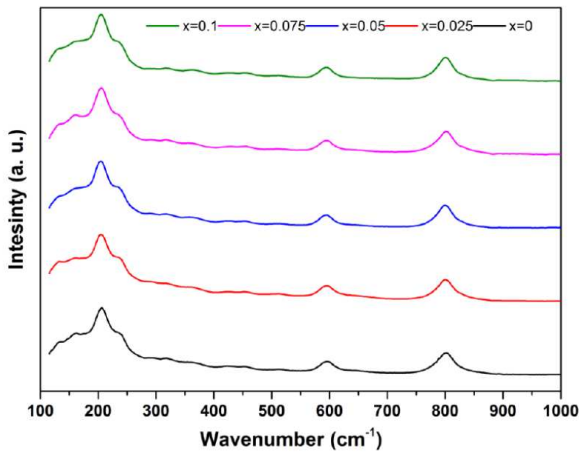

Figure 5. Raman spectra of Lu-doped $SrBi_2Ta_2O_9$ powders

temperature chemical stability in compounds is lower, e.g. bismuth might be readily volatilized. Relative density (i.e. the ratio of experimental density to theoretical density) increases with Lu-doping amount and reaches 96 %TD with the $SrBi_{1.9}Lu_{0.1}Ta_2O_9$ ceramics. The increase seems small in terms of the amount of dopant used, but they have consequences for the density of ceramics and their physical properties. Lu-doping had the task of improving ceramic density and reducing the loss of bismuth. Thus, higher relative density and lower material loss were achieved with sintering at 1200 °C for 1 h.

FTIR and Raman spectroscopies were used to probe different chemical bonds in a compound. As a function of the amount of dopant, both spectra are not only particularly smooth and sensitive to the amount of dopant introduced into a lattice structure, but also show the same chemical bond nature. Regarding FTIR spectra (Fig. 2), bands observed at around 556, 646 and 787 cm^{-1} are characteristic for $SrBi_2Ta_2O_9$ structure [1,13–15]. The absorption peaks at 3425 and 1632 cm^{-1} correspond to O–H stretching and bending modes of chemisorbed water. The peaks at 2924 and 2849 cm^{-1} could be assigned to the C–H stretching vibrations arising from traces of organic matter. The peak observed at 1384 cm^{-1}, which is more intense with some compounds, may be due to the carbonate group's improper decomposition in KBr [16].

Raman spectra of the Lu-doped $SrBi_2Ta_2O_9$ powders are illustrated in Fig. 3 and exhibit characteristic bands at approximately 168, 206, 595 and 801 cm^{-1} as well as at 321, 369 and 456 cm^{-1} [17,18]. The bands at ~805 and ~600 cm^{-1} are attributed to the oxygen stretching in O–Ta–O bonds in the TaO_6 octahedron. The band located at ~212 cm^{-1} is associated with the rock salt structure of Sr–O. The band at ~163 cm^{-1} is associated with the vibration of the Ta^{5+} ion along the *z*-direction within the TaO_6 octahedron [19,20].

FTIR and Raman results show that there are no significant changes in intensities of characteristic bands as a function of the dopant content. Atoms in crystals behave like springs and in a certain respect, the amount of dopant can sometimes only slightly affect interatomic vibrations. Consequently, no significant interatomic shifts were observed from the vibrational spectra.

Figure 4 shows fractured surfaces of the Lu-doped $SrBi_2Ta_2O_9$ ceramics sintered at 1200 °C for 1 h. The SEM reveals a general distinction between the undoped and doped samples. The undoped sample exhibits plate-

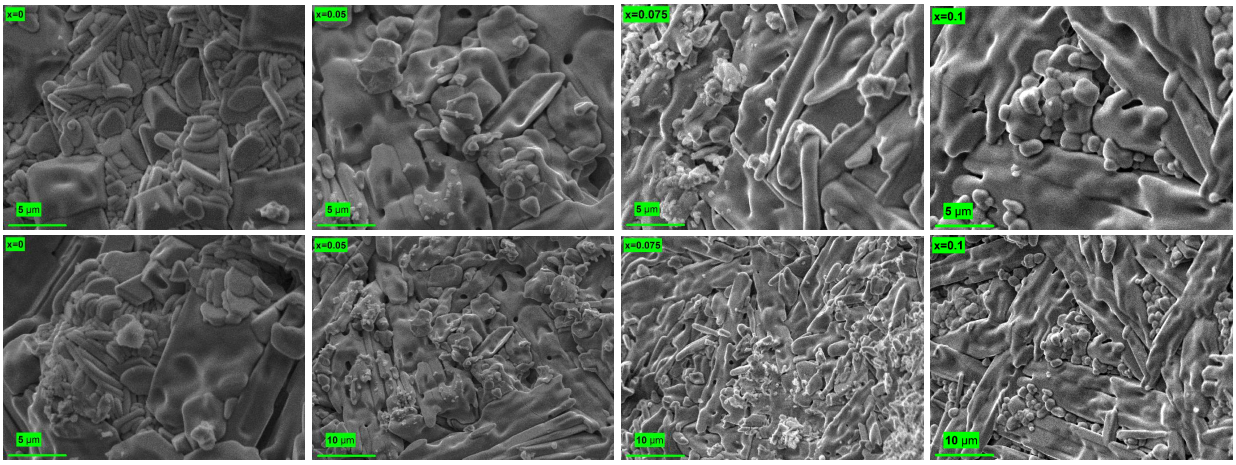

Figure 4. SEM images of Lu-doped $SrBi_{2-x}Lu_xTa_2O_9$ ceramics with different *x*

like morphology. Conversely, the doped ceramics had highly irregularly-shaped morphology and grain size did not vary significantly. Meanwhile, their microstructure is composed of both fine and coarse-grained particles. The relationship between Lu amount and grain size is less consistent. It would, on the whole, be affected by sintering conditions. Thus, during compaction and sintering, grain growth was obviously creating a coarser grain structure with several smaller particles filling the space between coarse grains and giving rise to porosity.

3.2. Dielectric properties

Comparisons of the dielectric constant (ε') and dielectric loss ($\tan\delta$) values of the Lu-doped $SrBi_2Ta_2O_9$ ceramics measured at V_{AC} = 0.1 V and V_{DC} = 0 V are given in Fig. 5. The dielectric constant was found to be as high as $\varepsilon \sim 267$ above 1 kHz for the $SrBi_{1.9}Lu_{0.1}Ta_2O_9$ (i.e. for $x = 0.1$), a value comparable to that of the undoped sample. The ceramics having $x = 0.025$ displayed the lowest ε' of ~244. However, the dielectric constant above 1 kHz was the highest (~277) for the sample $SrBi_{1.95}Lu_{0.05}Ta_2O_9$ and at the same time this ceramics (together with the undoped sample) had a minimal $\tan\delta$. Adding an ion of the same valence state usually does not increase the carrier concentration. However, in the case of the samples having $x = 0.05$ and $x = 0.1$, it seems that substituting Lu^{3+} ions at the Bi^{3+} site in $SrBi_2Ta_2O_9$ decreased the carrier concentration, leading to a high ε'. In addition, the Lu ion substitution did not drastically reduce $\tan\delta$ to less than 10^{-3}.

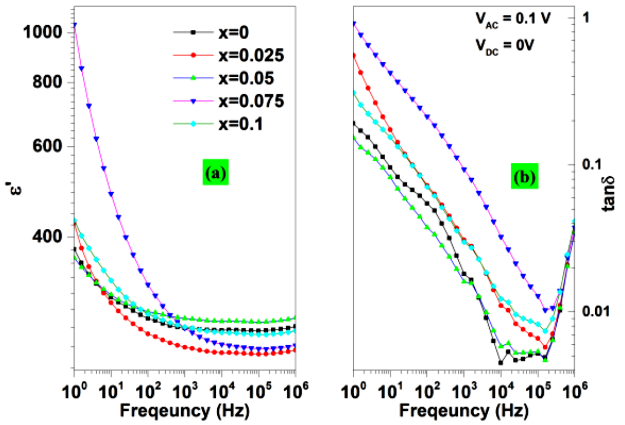

Figure 5. Comparison of ε' and $\tan\delta$ values of different Lu-doped $SrBi_2Ta_2O_9$ ceramics measured at V_{AC} = 0.1 V and V_{DC} = 0 V

Dielectric constant (ε') and dielectric loss ($\tan\delta$) of the prepared ceramics are independent on DC bias, as shown in Fig. 6. None of the compounds exhibited ε' and $\tan\delta$ degradation over the full DC range and did not result in any immediate change regarding ε'. Without a DC voltage, spontaneous polarization can happen freely. However, when a DC voltage was applied, spontaneous polarization was tied to the direction of the electric field in the dielectrics and independent reversal of spontaneous polarization was inhibited. As a result, $\tan\delta$ becomes lower than before applying the bias. In an ideal capacitor, as the frequency increases, ε' will tend to be constant, but here, there exists a frequency boundary beyond which the dielectric constant (ε') and dielectric loss ($\tan\delta$) smoothly rise again at higher frequency. Meanwhile, a rapid decrease in the dielectric constant with increasing frequency may be attributed to the reduction of the space charge polarization effect [21].

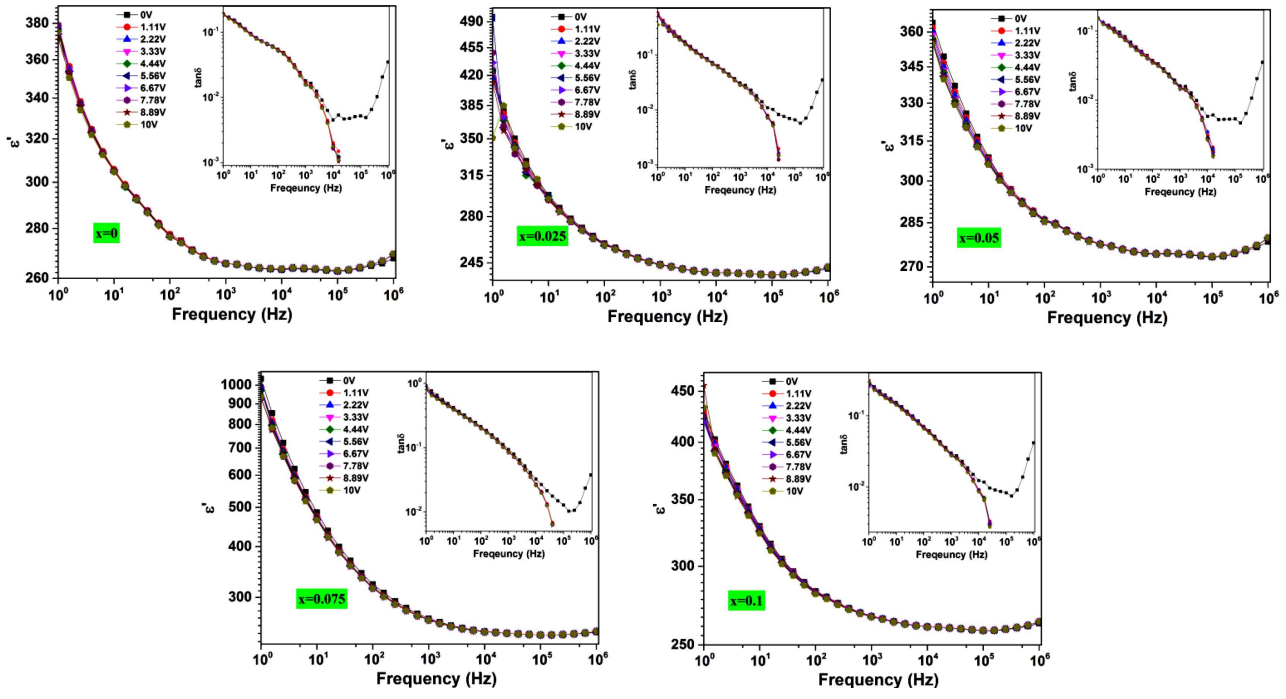

Figure 6. Dielectric constant (ε') and dielectric loss ($\tan\delta$) as a function of frequency and bias voltage of Lu-doped $SrBi_{2-x}Lu_xTa_2O_9$ ceramics with different x: a) 0, b) 0.025, c) 0.05, d) 0.075 and e) 0.1

According to experimental results, neither ε' nor $\tan\delta$ of the undoped and doped $SrBi_2Ta_2O_9$ compounds have a linear dependence on the dopant concentration. Three reasons might be responsible for this behaviour. The first is directly related to polarizability as a dominant factor. Bi^{3+} ions possess the highest polarizability which is strongly responsible for the increase of ε'. The second reason is the possibility of substituting Sr^{2+} (1.12 Å) with Lu^{3+} (0.85 Å) where Lu^{3+} ions might preferentially occupy Sr^{2+} sites at low doping concentrations and start to occupy Bi^{3+} sites when the Lu^{3+} concentration increases. The third reason could be the influence of grain size heterogeneity.

Both the dielectric constant (ε') and dielectric loss ($\tan\delta$) as a function of temperature for different frequencies are shown in Fig. 7. The dielectric constant of the undoped and doped samples is independent of frequency in the temperature range up to 280 °C, and then shows pronounced frequency dependence. All doped samples exhibit the ferroelectric-paraelectric transition of normal ferroelectric materials, like the pure $SrBi_2Ta_2O_9$, coupled with a broad peak indicating on a diffuse phase transition. The pure $SrBi_2Ta_2O_9$ sample has transition temperature around 300 °C. On the other hand, somewhat lower transition temperature of about 280 °C is characteristic of the doped samples. The decrease of the Curie temperature may be due to the absence of the lone pair of electrons on Lu^{3+} ion when compared to Bi^{3+} ion. The relatively high transition temperature of $SrBi_2Ta_2O_9$ is caused by the presence of bismuth atoms, which resonate with relatively high frequency within the crystal lattice. Because Lu is heavier than Bi, it resonates more slowly, so lower transition temperatures are expected for the doped samples.

Overall, an increase in temperature led to an increase in dielectric loss ($\tan\delta$) due to the increase in carrier concentration. It is evident that $\tan\delta$ increases smoothly in the temperature range 40–200 °C, and has values up to 10^{-2}. At higher temperatures, dielectric loss increases and this trend sped up from 280 °C.

In ferroelectric materials, the Curie Weiss's law illustrates the temperature dependence of the dielectric constant above the Curie temperature:

$$\frac{1}{\varepsilon'} = \frac{T - T_{CW}}{C} \tag{1}$$

where C and T_{CW} are the Curie constant and Curie-Weiss temperature, respectively. The Curie-Weiss plot is presented in Fig. 8. The transition between a low and high Curie temperature form of the pure and doped $SrBi_2Ta_2O_9$ ceramics is a second-order transition. This second-order transition begins at the point of intersection of the dashed lines, which represent the fitted linear regression curve. Meanwhile, the Curie constant of all compounds, whose order of magnitude is estimated to be around 10^5 °C^{-1}, is characteristic of displacive phase transitions. The doped samples show much larger deviations from ideal behaviour than the undoped one. This can be seen from the variation in temperature between T_C and T_{CW}.

The symmetry-breaking at the Curie temperature results in a phase transition to a higher symmetry phase, which is attributed to the well-known orthorhombic-to-tetragonal phase transition and consistent with a second-order transition.

As the Lu content increases in the specimens, disorderliness increases, leading to a diffuse phase tran-

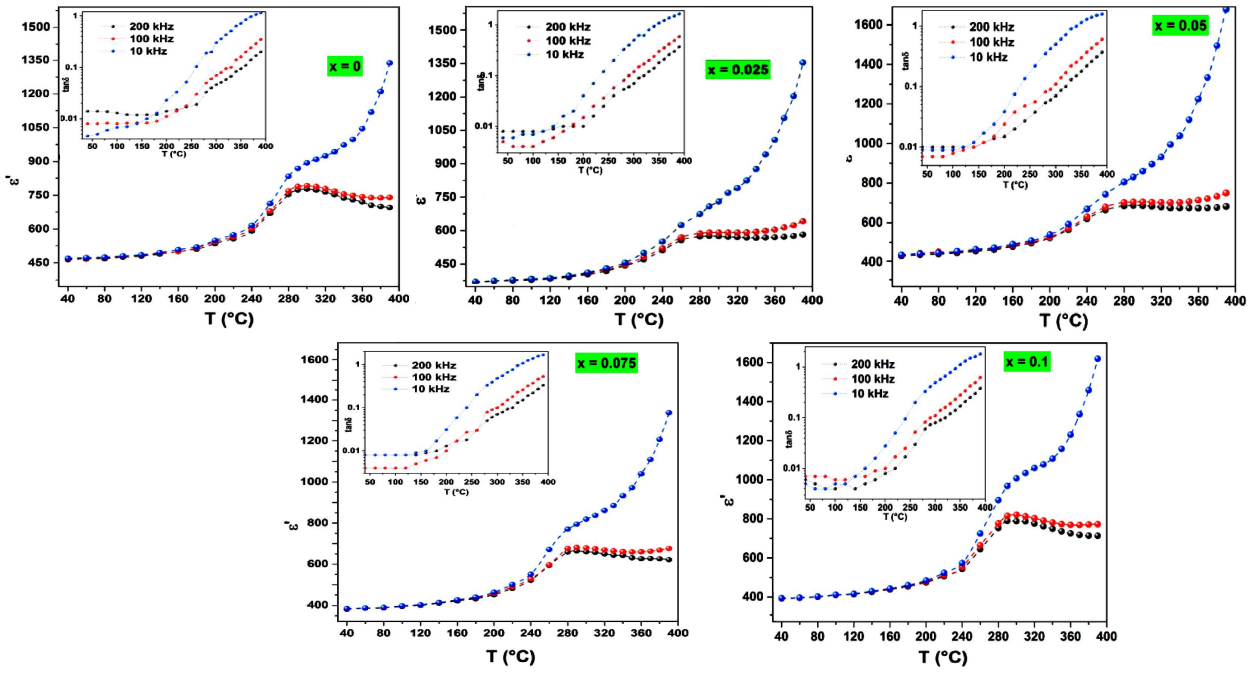

Figure 7. Dielectric constant (ε') and the dielectric loss ($\tan\delta$) of temperature-frequency-dependent Lu-doped $SrBi_{2-x}Lu_xTa_2O_9$ ceramics with different x: a) 0, b) 0.025, c) 0.05, d) 0.075 and e) 0.1

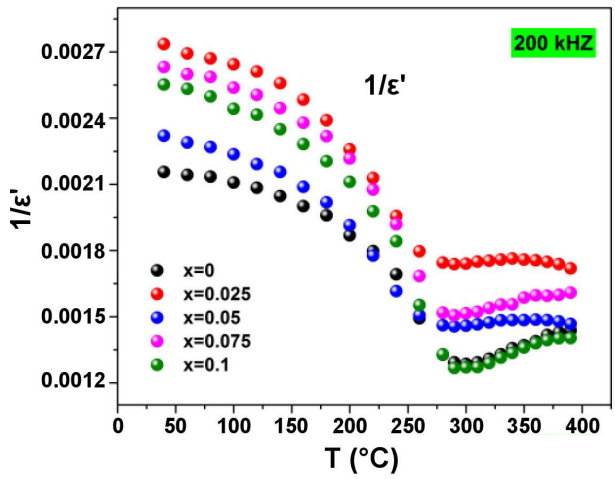

Figure 8. Reciprocal dielectric constant versus temperature at 200 kHz of Lu-doped $SrBi_2Ta_2O_9$ ceramics

sition [22]. Based on the structural characterization of the samples sintered at 1200 °C for 1 h and possible volatilization of bismuth, it was determined that the increase in dielectric diffuseness around the Curie temperature, may not be attributed only to the rise in charge defects within the lattice structure, but also to a reduction in grain size while the Lu amount rises.

The AC conductivity as a function of temperature at different frequencies of the Lu-doped $SrBi_2Ta_2O_9$ ceramics is shown in Fig. 9. Up to 180 °C, the conductivity increases smoothly and after 200 °C it increases steadily. As the temperature increases, the charge carriers can move among the lattice structure, and as a result, these carriers may be thermally activated when the temperature reaches 200 °C. The increase in conductivity with an increase in temperature confirms the NTCR (negative temperature coefficient of resistance [23]) behaviour of the materials laying down the conduction process arising from space charge conduction.

AC conductivity as a function of temperature was analysed using the Arrhenius equation:

$$\sigma_{AC} = \sigma_0 \cdot \exp\left(-\frac{E_a}{k \cdot T}\right) \tag{2}$$

where σ_0, E_a and k are temperature-independent constants, activation energy and the Boltzmann constant, respectively. The activation energy value was deduced from the slope of $\ln \sigma_{AC}$ versus $1000/T$. The activation energies at 200 kHz, over a temperature range of 240–290 °C, were estimated to be 1.33, 1.09, 1.03, 1.59 and 1.97 eV for x = 0, 0.025, 0.05, 0.075 and 0.1, respectively. For x = 0.025 and x = 0.05 the AC conductivities were 3.45×10^{-4} S/m and 4.14×10^{-4} S/m, respectively, when measured at 280 °C and 200 kHz. When comparing the activation energies of the Lu-doped $SrBi_2Ta_2O_9$ compounds, the x = 0.1 sample exhibited the highest activation energy, 1.97 eV, which is 1.48 and 1.23 times higher than that of the x = 0.05 and the undoped samples, respectively. As a result, the larger the Lu amount within the lattice is, the more energy is required to counter the thermal fluctuations of excited charge carriers at a selected temperature range. However, when a small amount of Lu is introduced into the structure, lower activation energy is obtained. This is due to a variety of factors, including a change in grain size and an increase in Sr-site disorder (Sr^{2+}, Bi^{3+}, and Lu^{3+} ions)

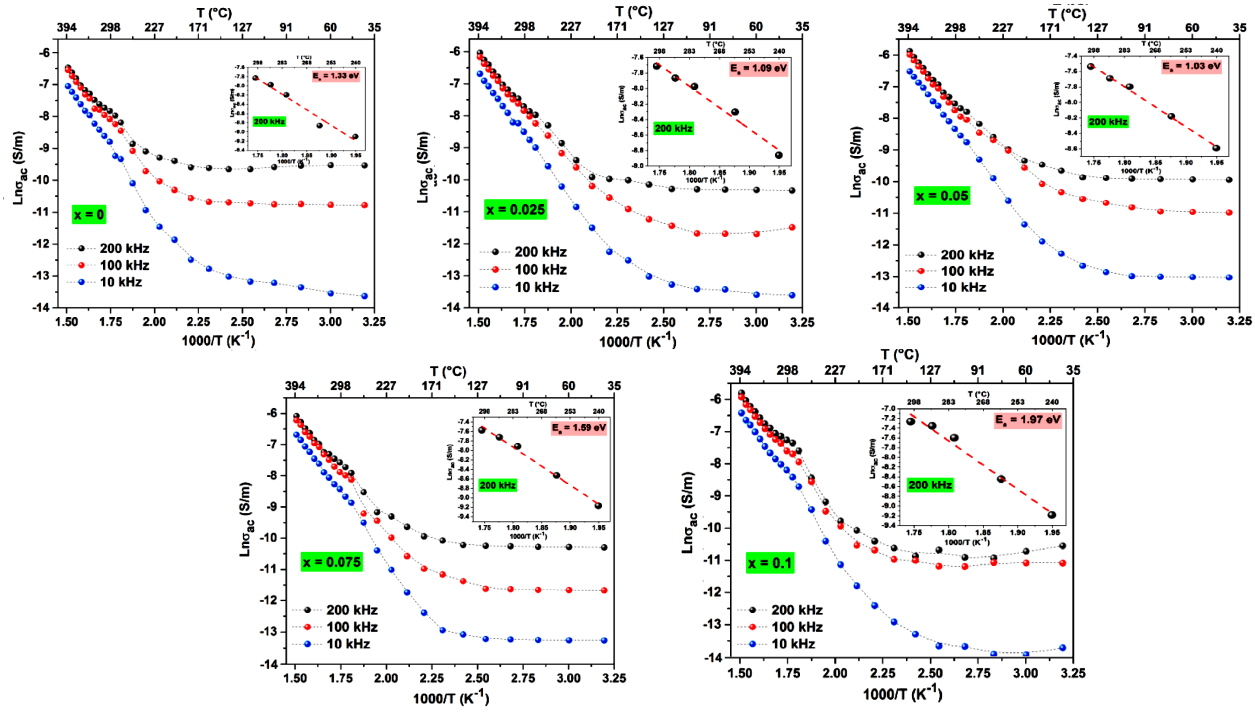

Figure 9. Frequency and temperature dependence of AC conductivity of Lu-doped $SrBi_{2-x}Lu_xTa_2O_9$ ceramics with different x: a) 0, b) 0.025, c) 0.05, d) 0.075 and e) 0.1

in the Bi_2O_2 and perovskite layers with variable Lu content. The smaller ion in the case of Lu^{3+} (0.848 Å [18]) provides more space, which promotes the ionic displacement. In other words, the higher activation energy is attributable to the lower bottleneck size for oxide-ion migration, but also possible existence of charge-clusters, that may arise from the introduction of Lu ions. A group of charges clustered together would lead to an increase in the activation energy in the substituted compounds [8].

Jumping from one side to the other, the hopping charge carrier has to overcome the activation energy. Meanwhile, a composition gradient in materials induces a chemical potential gradient, giving rise to activation energy as temperature increases.

The average AC conductivity, nearly 1.04×10^{-4} S/m, in the doped samples rose gradually, equal to the undoped one when measured at 200 °C at 200 kHz. By contrast, AC conductivity for all samples accounted for most of that increase with the contribution of dopants, there is around 2.8×10^{-4} S/m for $x = 0$ and 5.2×10^{-4} S/m for $x = 0.1$ when measured at 280 °C and the same frequency. This inverted AC conductivity at high temperatures might either be attributed to the fact that the more diffuseness is pronounced, higher the conductivity will be, or the closer the Curie temperature is, higher the charge carrier density will be leading to increased AC conductivity.

IV. Conclusions

Lu-doped $SrBi_2Ta_2O_9$ ($SrBi_{2-x}Lu_xTa_2O_9$ where x = 0, 0.025, 0.05, 0.75 and 0.1) compounds were synthesized by combination of molten salt method and solid-state route and sintering at different temperatures up to 1200 °C. The prepared samples had pure and single-phase orthorhombic structure with plate-like morphology that is composed of fine and coarse-grained particles.

It was shown that the sample $SrBi_{1.95}Lu_{0.05}Ta_2O_9$ had maximal dielectric constant (ε') and minimal dielectric loss ($\tan\delta$). The prepared samples demonstrated their normal ferroelectric behaviour. The ferroelectric-paraelectric transition is coupled with a broad peak indicating on a diffuse phase transition. The pure $SrBi_2Ta_2O_9$ sample had transition temperatures around 300 °C, however, somewhat lower transition temperature of about 280 °C was characteristic of the doped samples.

There was no linear dependence of the dielectric properties on the Lu content. Thus, it was impossible to determine whether ceramics heterogeneity or Lu substitution was the exact reason for different values of dielectric constant and dielectric loss.

References

1. V. Senthil, T. Badapanda, A. Chandra Bose, S. Panigrahi, "Relaxation and conduction mechanism of Dy^{3+} substituted $SrBi_2Ta_2O_9$ ceramics", *J. Mater. Sci. Mater. Electron.*, **27** (2016) 4760–4770.
2. C. A-Paz de Araujo, J.D. Cuchiaro, L.D. McMillan, M.C. Scott, J.F. Scott, "Fatigue-free ferroelectric capacitors with platinum electrodes", *Nature*, **374** (1995) 627–629.
3. N. Li, Q. Zhu, G. Liu, Q. Zhao, H. Lv, M. Yuan, Q. Meng, Y. Zhou, J. Xu, C. Wang, "Modulation of photocatalytic activity of $SrBi_2Ta_2O_9$ nanosheets in NO removal by tuning facets exposure", *J. Mater. Sci. Technol.*, **122** (2022) 91–100.
4. M. Zhu, B. Liao, Y. Tang, X. Chen, R. Ma, L. Li, X. Fan, "The superior piezocatalytic performance of $SrBi_2Ta_2O_9$ nanoflower : Mechanism of screening effect and energy band theory", *Appl. Surf. Sci.*, **628** (2023) 157366.
5. M. Afqir, M. Elaatmani, A. Zegzouti, N. Tahiri, M. Daoud, "Molten salt synthesis , structural and dielectric properties of $SrBi_{2-y}Y_yNb_{2-x}V_xO_9$ ($0 \le x \le 0.2$ and $0 \le y \le 0.2$) ceramics", *J. Electron. Mater.*, **51** (2022) 3863–3872.
6. M. Afqir, M. Elaatmani, A. Zegzouti, N. Tahiri, M. Daoud, "Molten salt synthesis of Gd-doped $SrBi_2Ta_2O_9$ ceramics with enhanced dielectric properties at room temperature", *Appl. Phys. A*, **128** (2022) 832.
7. T.P. Wendari, M. Ikhram, Y.E. Putri, U. Septiani, "Enhanced dielectric and ferroelectric responses in La^{3+}/Ti^{4+} co-substituted $SrBi_2Ta_2O_9$ Aurivillius phase", *Ceram. Int.*, **48** (2022) 10328–10332.
8. V. Senthil, S. Panigrahi, "Dielectric, ferroelectric, impedance and photocatalytic water splitting study of Y^{3+} modified $SrBi_2Ta_2O_9$ ferroelectrics", *Int. J. Hydrogen Energy*, **44** (2019) 18058–18071.
9. Y. Zhong, B. Deng, X. Gao, P. Sun, Y. Ren, T. Liang, R. Yu, "High thermally Sm^{3+}-activated $SrBi_2Ta_2O_9$ orange-red phosphor: Preparation, characterization, and optical properties", *J. Lumin.*, **215** (2019) 116648.
10. Y. Zhong, P. Sun, X. Gao, Q. Liu, S. Huang, B. Liu, B. Deng, R. Yu, "Synthesis and optical properties of new red-emitting $SrBi_2Ta_2O_9:Eu^{3+}$ phosphor application for w-LEDs commercially based on InGaN", *J. Lumin.*, **212** (2019) 45–51.
11. M. Afqir, A. Tachafine, D. Fasquelle, M. Elaatmani, J.C. Carru, A. Zegzouti, M. Daoud, "Dielectric properties of $SrBi_{1.8}RE_{0.2}Nb_2O_9$ (RE = Yb, Tm, Tb, Gd, Er, Sm and Ce) ceramics", *Solid State Sci.*, **73** (2017) 51–56.
12. M. Afqir, A. Tachafine, D. Fasquelle, M. Elaatmani, J.-C. Carru, A. Zegzouti, M. Daoud, "Dielectric properties of gadolinium-doped $SrBi_2Nb_2O_9$ ceramics", *J. Mater. Sci. Mater. Electron.*, **29** (2017) 1289–1297.
13. H. Ke, Y. Zhou, D.C. Jia, W. Wang, X.Q. Xu, F. Ye, "Crystallization and nanograin growth in $SrBi_2Ta_2O_9$ synthesized by a novel sol-gel process", *J. Sol-Gel Sci. Technol.*, **34** (2005) 131–136.
14. M. Moret, R. Zallen, R. Newnham, P. Joshi, S. Desu, "Infrared activity in the Aurivillius layered ferroelectric $SrBi_2Ta_2O_9$", *Phys. Rev. B*, **57** (1998) 5715–5723.
15. C.H. Lu, S.K. Saha, "Synthesis of ultrafine strontium bismuth tantalate powder by colloid-emulsion technique", *Mater. Lett.*, **42** [3] (2000) 150–154.
16. F. Cao, J. Chen, M. Ni, H. Song, G. Xiao, W. Wu, X. Gao, K. Cen, "Adsorption of NO on ordered mesoporous carbon and its improvement by cerium", *RSC Adv.*, **4** (2014) 16281–16289.
17. S. Kojima, I. Saitoh, "Soft phonon and bismuth content in ferroelectric $SrBi_2Ta_2O_9$", *Phys. B Condens. Matter*, **263-264** (1999) 653–656.

18. C.C. Wu, C.F. Yang, "Effect of V_2O_5 B-site substitution on the microstructure, Raman spectrum, and dielectric properties of $SrBi_2Ta_2O_9$ ceramics", *Sci. Rep*., **10** (2020) 1–14.
19. W. Perez, R.R. Das, P.S. Dobal, Y.I. Yuzyuk, P. Bhattacharya, R.S. Katiyar, "Effect of cationic substitution on Raman spectra of $SrBi_2Ta_2O_9$ ceramics and thin films", *Mater. Res. Soc. Symp. Proceed*., **784** (2003) 139–144.
20. R. Liu, P. Han, "Lattice vibrational properties of $SrBi_2Ta_2O_9$", *MRS Proceed*., **655** (2000) 404–409.
21. C.-S. Hong, S.-Y. Chu, C.-C. Tsai, W.-C. Su, "Manganese effect on the relaxation behaviors of the space charge polarization in $Pb(Fe_{2/3}W_{1/3})_{0.9}Ti_{0.1}O_3$ ceramics", *Ceram. Int*., **37** (2011) 3405–3411.
22. D. Dhak, P. Dhak, T. Ghorai, P. Pramanik, "Dielectric diffuseness and conductivity study of $CuNb_2O_6$ incorporated $BaTiO_3$ synthesized by chemical route", *J. Appl. Phys.*, **102** (2007) 074117.
23. X. Li, X. Chen, N. Wei, W. Kong, B. Gao, "Investigation of pyrochlore-type $A_2Sn_2O_7$ (A = La, Nd, Sm, or Gd) ceramics as negative temperature coefficient thermistors for high-temperature application", *J. Phys. Chem. Solids*, **175** (2023) 111205.